Rare Metal Materials and Engineering
Volume 48, Issue 1, January 2019
Available online at www.rmme.ac.cn

Science Press

Cite this article as: Rare Metal Materials and Engineering, 2019, 48(1): 0039-0043.

ARTICLE

Silicon Oxycarbide Powders Doped with in Situ Grown SiC Nanowires: Synthesis and Dielectric Properties

Ye Fang, Duan Wenyan, Mo Ran, Yin Xiaowei, Zhang Litong, Cheng Laifei

Science and Technology on Thermostructural Composite Materials Laboratory, Northwestern Polytechnical University, Xi'an 710072, China

Abstract: The amorphous silicon oxycarbide powders containing in situ grown single-crystal silicon carbide nanowires were fabricated via the pyrolysis of a polymeric precursor using ferrocene as the catalyst. The nanowires, with lengths of several micrometers and diameters of 10~100 nm, were composed of single-crystal β-SiC along the <111> growth direction and uniformly dispersed in the composite powders. The growth mechanism of silicon carbide nanowires was explored by analyzing the microstructure of the silicon carbide nanowires. The dielectric properties of the composite ceramic powders were studied. The results demonstrates that silicon carbide nanowires can be used to adjust the electrical property of the composite, and a high nanowire content can result in a large real and imaginary part of permittivity.

Key words: silicon oxycarbide; in situ grown sic nanowire; growth mechanism; dielectric property

One-dimensional nanomaterials, such as nanotubes and nanowires, have attracted more and more attention due to their unique structures and properties. These materials are of great interests for the possibility to adjusting their mechanical[1,2], electrical[3,4] and magnetic[5] properties and many applications ranging from probe microscopy tips to interconnections in nanoelectronics[6,7]. As an intrinsic n-type semiconductor, silicon carbide (SiC) outperforms other materials such as silicon in electronic devices for high-power, high-frequency and high-temperature applications[8]. SiC nanowires exhibit weak gating effect, low resistivity, and very low electron mobility, which may be ascribed primarily to the one-dimensional carrier confinement in the nanowires[9]. Furthermore, the high strength and stiffness of SiC nanowires combined with a high aspect ratio make them a very effective reinforcement for various composites[10].

Recently, great progress has been made in the synthesis of SiC nanowires. Such as carbon nanotube-confined reaction[11], laser ablation[12], chemical vapor deposition (CVD)[13], advanced carbothermal reduction of silica xerogels[14]. Despite the wide variety of techniques for growing SiC nanowires, most of them can be described by vapor-liquid-solid (VLS)[15,16] and vapor-solid (VS)[17] mechanisms. The VLS mechanism involves the use of liquid catalysts to act as the energetically favored site for the absorption of silicon and carbon species from the surrounding gases to grow nanowires. These nanowires are easily recognized by the iron-rich semispherical nanowire tip. But the nanowire tip is sharp in the VS mechanism.

However, previous researches have shown that the inhomogeneous distribution of the preformed nanowires in the final product limits the potential benefits of the physical properties of SiC nanowires as reinforcements. The development of processing technique to achieving uniform dispersion within nanoscale matrices for successful use of these materials is still a significant challenge. One way to overcome the above-mentioned issues is to process with composite powders that contain in situ formed reinforcing nanophases[18,19]. Polymer-derived ceramics synthesized by thermal decomposition of polymeric ceramic precursors have attracted extensive attention. It has been demonstrated

Received date: June 25, 2018
Foundation item: National Natural Science Foundation of China (51602258, 51502242, 51725205, 51332004); Natural Science Basic Research Plan in Shaanxi (2017JM5094).
Corresponding author: Ye Fang,Ph. D.,Associate Professor , Science and Technology on Thermostructural Composite Materials Laboratory, Northwestern Polytechnical University, Xi'an 710072, P. R. China, Tel: 0086-29-88495163, E-mail: yefang511@nwpu.edu.cn

that these materials have many advantages over the traditional ceramics in terms of processing, properties, and forming capability.

In this paper, we report the synthesis of novel composite powders containing amorphous silicon oxycarbide (SiOC) powders and in situ grow single-crystal SiC nanowires through the pyrolysis of a polymer precursor using ferrocene as the catalyst. The unique characteristic of this method is that the SiOC powders and SiC nanowires can be formed simultaneously. SiC nanowires can be used to adjust the electrical properties of the composite, which is important to control the dielectric properties of the composite.

1 Experiment

Polysiloxane (PSO) was used as the precursors. It was supplied by graduate university of Chinese academy of science, Beijing, China. Ferrocene ($Fe(C_5H_5)_2$, purity≥99%) was used as a catalyst. Firstly, the PSO with 5 wt% ferrocene was mixed at 80 °C for 30 min in an Ar atmosphere. Then a transparent orange liquid was obtained. The precursor was cross-linked at 300 ºC for 2 h in an argon atmosphere. The cross-linked product was then ball milled for 12 h and passed through a 74 μm sieve. The powder mixture was then placed in a high-purity alumina crucible and pyrolyzed in a conventional furnace under the flowing Ar atmosphere. Thereafter, the powder mixture was heated to 1450 °C at a heating rate of 5 °C/min and held for 4 h followed by furnace cooling.

The morphology and microstructure of the composite ceramic were observed by scanning electron microscopy (SEM, S-2700, Hitachi, Japan) and transmission electron microscope (TEM, G-20, FEI-Tecnai, Hillsboro, U.S.A.) equipped with energy dispersive spectrum (EDS) by a Cu grid as the sample holder. The phase compositions of the SiO_2-SiC ceramic were analyzed by X-ray diffraction (XRD, Rigaku-D/max-2400, and Tokyo, Japan). The relative complex permittivity of samples was measured in the frequency range of 8.2~12.4 GHz (X band) using a vector network analyzer (VNA, MS4644A, Japan). The samples used for dielectric properties measurement were prepared by mixing the nanocomposite powders with paraffin and then pressed into special shapes with a dimension of 22.86 mm × 10.16 mm × 1.5 mm. The mass ratio of powders to paraffin were 1:9, 3:7, 5:5, 7:3 and 9:1.

2 Results and Discussion

Fig. 1a shows SEM morphology of the as-synthesized powder (the pyrolysis product), consisting of irregular-shaped particles and nanowires. Note that the SiC nanowires are uniformly dispersed in the SiOC matrix. The diameter of SiC nanowires ranges from 10 nm to 100 nm and the length is over several micrometers. And spherical metal catalysts was found on the tips of SiC nanowires. This is attributed to Fe playing the role of metal catalyst for the formation of SiC one-dimensional structure. Fig. 1b shows the XRD pattern of the synthesized powders. The sample displays a broad hump in the 20°~30° range (2θ) belonging to an amorphous SiC_xO_y phase and shows the crystalline peaks at 2θ of 35.6º, 41.4°, 60.0º, 71.8º and 45.3°, which refer to the diffractions from the (111), (220), (200) and (311) lattice planes of β-SiC (JCPDS Card no. 29-1129) and the (210) lattice planes of FeSi (JCPDS Card no. 28-1397), respectively.

TEM and high resolution TEM (HRTEM) images recorded on the powders a provide further insight into the structure of the composite ceramic. Fig. 2a reveals the powder morphologies containing particles and nanowires. The EDS spectra of A and B zones marked in Fig.2a (Fig. 2b and 2c) show that the particles consist only of silicon, carbon and oxygen atoms. Typical HRTEM images of the particles and nanowires are shown in Fig.3a and 3b, respectively. It reveals that the particles contain nanocrystalline SiC, and a little amorphous SiOC. The HRTEM image and corresponding SAED patterns of nanowires (inset of Fig. 3) show that the nanowires consist of a single crystal β-SiC core structure and a very thin amorphous shell coating. The core crystal nanowire has a diameter of 10~100 nm, and possesses high-density stacking faults in the crystal plane normal to the axis of the nanowire. These stacking faults are generally thought to originate from thermal stress during the growth process[20, 21]. The distance between these planes is 0.25 nm that is the same as the distance between the {111} planes in β-SiC crystalline. The SAED patterns are always perpendicular to the stacking fault

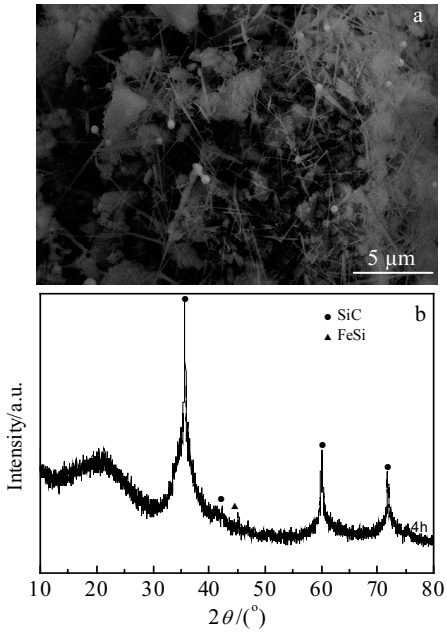

Fig. 1 SEM image (a) and XRD pattern (b) of the synthesized powders

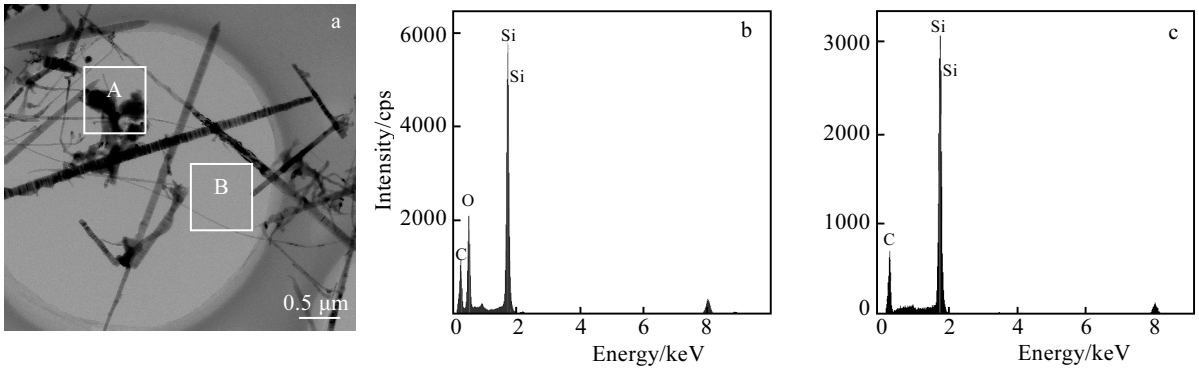

Fig.2 TEM image of the composite ceramic (a) and the typical EDS spectra of A (b) and B (c) zones marked in Fig.2a

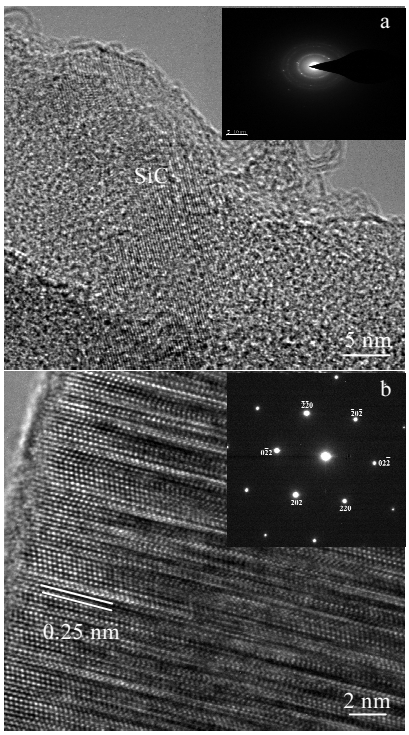

Fig.3 HRTEM images and SAED patterns of A (a) and B (b) zones marked in Fig.2a

planes{111}, and the main growth direction of the nanowires can be judged as parallel to the <111> direction.

In reality, SiC nanowires are synthesized by the carbothermal reduction reaction according to the overall reaction as follows [22,23]:

$$SiO_2 + C \rightarrow SiC + CO_2 \quad (1)$$

Reaction (1) cannot be completed in one step but involves a multiple-step process. It includes reactions (2)~(6).

$$SiO_2 + C \rightarrow SiO + CO \quad (2)$$

$$SiO_2 + CO \rightarrow SiO + CO_2 \quad (3)$$

$$CO_2 + C \rightarrow 2CO \quad (4)$$

$$SiO + 2C \rightarrow SiC + CO \quad (5)$$

$$SiO + CO \rightarrow SiC + CO_2 \quad (6)$$

Reaction (6) is followed by reaction (4) to synthesize CO, which in turn reacts with SiO_2 and SiO according to reaction (3) and reaction (6), respectively, and then the cycle continues. SiC can be prepared by uniform nucleation according to reaction (5) with solid-gas interaction, but the growth of SiC nanowires is believed to experience a gas-gas reaction (6) [24-26].

Further advancement of this approach to nanowire synthesis requires a clear understanding of the growth mechanism. The presence of nanoparticles at one end of nearly all the nanowires suggests that our growth proceeds by a VLS mechanism. This idea can be tested and developed in more detail by considering of the model in Fig.4. In this model, when the temperature is high enough, the ferrocene is pyrolyzed into Fe atoms, subsequently the reaction between the silicon-containing vapors and Fe particles yields iron silicide, which agglomerates into droplets. The surface of the droplets is a preferred site for gas deposition because of

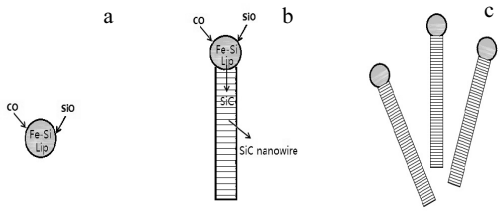

Fig.4 Proposed nanowire growth model: (a) the hot vapor condenses into small clusters, and the furnace temperature is controlled to maintain the FeSi nanocluster in a liquid state; (b) nanowire growth begins after the liquid becomes supersaturated with SiO and CO and continues as long as the FeSi nanoclusters remain in a liquid state and the SiO and CO reactants are available; (c) growth terminates when the nanowire passes out of the hot reaction zone (in the carrier gas flow) onto the cold finger and the FeSi nanoclusters solidify

its large accommodation coefficient[27] (Fig.4a), and when the nanoclusters become supersaturated with silicon- and carbon-carrying vapors and act as a reservoir for the reactants, the SiC phase forms. The SiC crystals diffuse and precipitate from the droplets due to the low solubility of SiC in Fe, which gives a rise to SiC nuclei. A liquid-solid interface is created on the surface of the liquid droplets once the SiC nuclei form. The dissolved Si and C atoms preferentially diffuse out through the droplets and stack on the existing liquid-solid interface because this process consumes less energy than that needed to form a new nucleation site within the droplets [28, 29]. The nanowires grow longer with more and more silicon- and carbon- carrying vapors dissolve in the droplets (Fig.4b). Ultimately, the growth terminates when the gas flow carries the nanowires out of the hot zone of the furnace (Fig. 4c) [30]. The precipitation drives the axial growth of the nanowires and pushes the liquid metal droplets away from the substrate along the direction of <111>, because the {111} surfaces of the face-centered cubic SiC structures have the lowest surface energy [31].

Fig. 5 illustrates the dielectric properties in X-band for the ceramic powders with different powder contents. As shown in Fig. 5a, 5b, with the increase of the powder content, both real part permittivity ε' and imaginary part permittivity ε'' increase across the whole X-band in the range

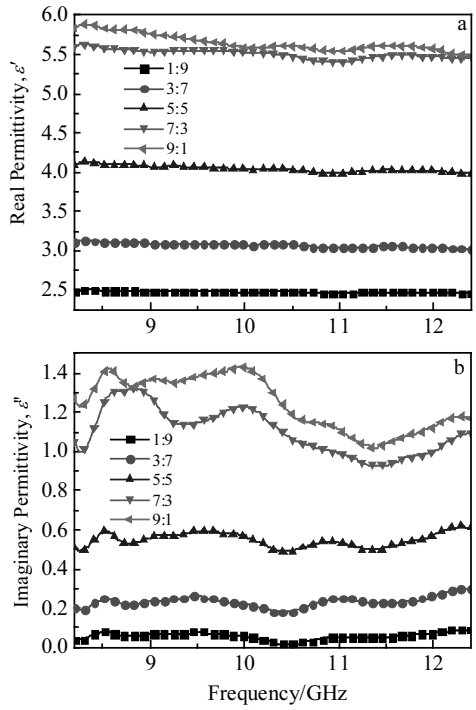

Fig. 5 Real permittivity (a) and the imaginary permittivity (b) of ceramics with different nanocomposite powder contents versus frequency

of 2.46~5.8 and 0.01~1.08, respectively. SiC nanowire has high carrier concentrations close to the metallic limit for a weak gating effect[32]. The confinement of carriers into one dimensional nanowires on a nanometer scale can greatly increase the carrier concentration. The content of SiC nanowires increases with the increase of ceramic powders. On the one hand, the increased SiC nanowire content leads to a larger nano-surface in the composite and a more developed network formed by the bridging between SiC nanowires, which gives a rise to the accumulation of charges at the surface, and leading to the interfacial electron polarization and the hopping of electrons in the network [33], with can be attributed to the conductive loss. On the other hand, considering the wire-like shape of SiC nanowires in the composites, they can act as "micro-antennae" to receive electromagnetic waves[34]. Both of them can result in a high dielectric constant.

3 Conclusions

1) A novel amorphous SiOC powders with in situ-grown single-crystal SiC nanowires were synthesized via the catalyst-assisted pyrolysis of a polymeric precursor.

2) The nanowires are uniformly dispersed within the SiOC powder. The powder mixtures are useful in the synthesis of nanowire-reinforced SiOC nanocomposites.

3) The presence of nanoparticles at one end of the nanowires suggests that the growth proceeds by a VLS mechanism. The real part and the imaginary part of permittivity increases with the increasing SiC nanowire content.

References

1 Fu Q G, Gu C G, Li H J *et al*. *Materials Science & Engineering A*[J], 2013, 563: 133

2 Chu Y H, Fu Q G, Li H J *et al*. *Journal of the American Ceramic Society*[J], 2012, 95: 739

3 Vrbanic D, Pejovnik S, Mihailovic D *et al*. *Journal of the European Ceramic Society*[J], 2007, 27: 975

4 Song Q, Yan H, Liu K *et al*. *Advanced Energy Materials*[J], 2018(8): 1 800 564

5 McHenry M E, Johnson F, Okumura H *et al*. *Scripta Materialia*[J], 2003, 48: 881

6 Alivisatos A P. *Science*[J], 1996, 271: 933

7 Yakobson B I, Smalley R E. *American Scientist*[J], 1997, 85: 324

8 Madar R. *Nature*[J], 2004, 430: 974

9 Seong H K, Choi H J, Lee S K *et al. Applied Physics Letters*[J], 2004, 85: 1255

10 Pozuelo M, Kao W H, Yang J M. *Materials Characterization*[J], 2013, 77: 81

11 Pan Z W, Lai H L, Au F C K *et al*. *Advanced Material*[J], 2000, 12: 1186

12 Zhang Y, Suenaga K, Colliex C *et al*. *Science*[J], 1998, 281:

973
13 Yang W, Araki H, Kohyama A *et al*. *Materials Letters*[J], 2004, 58: 3145
14 Liang C H, Meng G W, Zhang L D *et al*. *Chemical Physics Letters*[J], 2000, 329: 323
15 Selvam A, Nair N G, Singh P. *Journal of Materials Science Letters*[J], 1998, 17: 57
16 Li Y B, Xie S S, Zou X P *et al*. *Journal of Crystal Growth*[J], 2001, 223: 125.
17 Wei J, Li K Z, Chen J *et al*. *Journal of Crystal Growth*[J], 2011, 335: 160
18 Oh Y S, Kim C S, Lim D S *et al*. *Scripta Materialia*[J], 2001, 44: 2079
19 Xie Z P, Lu J W, Liu T *et al*. *Journal of Materials Science Letters*[J], 2001, 20: 1425
20 Li H J, Li Z J, Meng A L *et al*. *Journal of Alloys and Compounds*[J], 2003, 352: 279
21 Kang B C, Lee S B, Boo J H. *Thin Solid Films*[J], 2004, 464-465: 215
22 Greil P. *Advanced Engineering Materials*[J], 2000, 2: 339
23 Li X K, Liu L, Zhang Y X *et al*. *Carbon*[J], 2001, 39: 159
24 Xu T H, Ma Q S, Chen Z H. *Materials Science and Engineering A*[J], 2011, 530: 266
25 Meng G W, Zhang L D, Qin Y *et al*. *Nanostructured Materials*[J], 1999, 12: 1003
26 Meng G W, Cui Z, Zhang L D *et al*. *Journal of Crystal Growth* [J], 2000, 209: 801
27 Vakifahmetoglu C, Pippel E, Woltersdorf J *et al*. *Journal of the American Ceramic Society*[J], 2010, 93: 959
28 Li G Y, Li X D, Chen Z D *et al*. *The Journal of Physical Chemistry C*[J], 2009, 113: 17655
29 Yoon B H, Park C S, Kim H E *et al*. *Journal of the American Ceramic Society*[J], 2007, 90: 3759
30 Alfredo M M, Charles M L. *Science*[J], 1998, 279: 208
31 Wu R B, Zhou K, Wei J *et al*. *The Journal of Physical Chemistry C*[J], 2012, 116: 12 940
32 Seong H K, Choi H J, Lee S K *et al*. *Applied Physics Letters*[J], 2004, 85: 1255
33 Han M, Yin X, Hou Z *et al*. *ACS Applied Materials & Interfaces*[J], 2017(9): 11 803
34 Chen Y, Cao M, Wang T *et al*. *Applied Physics Letters*[J], 2004, 84: 3367

原位自生 SiC 纳米线掺杂 SiOC 陶瓷粉体的制备与介电性能

叶　昉，段文艳，莫　然，殷小玮，张立同，成来飞
(西北工业大学 超高温结构复合材料实验室，陕西 西安 710072)

摘　要：以二茂铁为催化剂，催化裂解陶瓷聚合物先驱体制备了原位自生 SiC 纳米线掺杂的 SiOC 陶瓷粉体。SiC 纳米线为堆垛方向为<111>的 β 相单晶体，直径为 10~100 nm，长度可达数微米，均匀分布在 SiOC 粉体中。基于 SiC 纳米线微观结构分析，探讨了纳米线的生长机制。研究了复合陶瓷粉体的介电性能。结果发现，SiC 纳米线含量可调控复合粉体的电性能，较高含量纳米线可赋予复合粉体较高的介电实部与虚部。

关键词：SiOC陶瓷；原位自生SiC纳米线；生长机制；介电性能

作者简介：叶 昉，女，1984 年生，博士，副教授，西北工业大学超高温结构复合材料实验室，陕西 西安 710072，电话：029-88495163，E-mail: yefang511@nwpu.edu.cn